

See discussions, stats, and author profiles for this publication at: <https://www.researchgate.net/publication/5392809>

Residue-Level Interrogation of Macromolecular Crowding Effects on Protein Stability

ARTICLE *in* JOURNAL OF THE AMERICAN CHEMICAL SOCIETY · JUNE 2008

Impact Factor: 12.11 · DOI: 10.1021/ja8005995 · Source: PubMed

CITATIONS

50

READS

29

6 AUTHORS, INCLUDING:



Christopher Barnes

University of Pittsburgh

9 PUBLICATIONS 141 CITATIONS

SEE PROFILE



Conggang Li

Wuhan Institute of Physics and Mathematics

53 PUBLICATIONS 1,328 CITATIONS

SEE PROFILE



Jillian Orans

Duke University Medical Center

13 PUBLICATIONS 618 CITATIONS

SEE PROFILE

Published in final edited form as:

J Am Chem Soc. 2008 May 28; 130(21): 6826–6830.

Residue-Level Interrogation of Macromolecular Crowding Effects on Protein Stability

Lisa M. Charlton[†], Christopher O. Barnes[†], Conggang Li[†], Jillian Orans[†], Gregory B. Young[‡], and Gary J. Pielak^{*,†,‡,§}

[†] Department of Chemistry, University of North Carolina at Chapel Hill, Chapel Hill, North Carolina 27599

[‡] Department of Biochemistry and Biophysics, University of North Carolina at Chapel Hill, Chapel Hill, North Carolina 27599

[§] Lineberger Comprehensive Cancer Center, University of North Carolina at Chapel Hill, Chapel Hill, North Carolina 27599

Abstract

Theory predicts that macromolecular crowding affects protein behavior, but experimental confirmation is scant. Herein, we report the first residue-level interrogation of the effects of macromolecular crowding on protein stability. We observe up to a 100-fold increase in the stability, as measured by the equilibrium constant for folding, for the globular protein chymotrypsin inhibitor 2 (CI2) in concentrations of the cosolute poly(vinylpyrrolidone) (PVP) that mimic the protein concentration in cells. We show that the increased stability is caused by the polymeric nature of PVP and that the degree of stabilization depends on both the location of the individual residue in the protein structure and the PVP concentration. Our data reinforce the assertion that macromolecular crowding stabilizes the protein by destabilizing its unfolded states.

Introduction

Macromolecular crowding is predicted to stabilize proteins.¹ Even though proteins participate in every biochemical process and are used as therapeutics, we lack fundamental knowledge about crowding and protein stability. The consequences of macromolecular crowding are expected to be profound,¹ yet, surprisingly, most biophysical studies are conducted only in dilute solution. Quantitative information about the effects of crowding on globular proteins would not only provide new insights into intracellular constraints on protein stability but also help find formulations that increase the stability and facilitate the long-term storage of protein pharmaceuticals.

As protein function in the cell occurs at macromolecular concentrations of 300 g/L or greater,² relevant experiments must attempt to mimic this environment. Sequestering a protein in a biocompatible, protein-like polymer provides a simplified representation of the cellular interior that focuses on the potential stabilizing effect of steric repulsion.^{3,4} A study conducted by Minton and co-workers showed that crowding with dextran (mw 35 000 Da) increases the equilibrium constant for folding of the molten-globule state of cytochrome *c* by 100-fold at pH 2.0.⁴ This shows crowding can promote stabilization. These data, however, were acquired under extreme conditions, did not involve the native state of the protein, and focused on bulk rather than residue-specific measurements.

E-mail: gary_pielak@unc.edu.

Supporting Information Available: Experimental Procedures, Table S1, Figures S1–S4. This material is available free of charge via the Internet at <http://pubs.acs.org>.

Other studies of protein stability in the presence of macro-molecules have reported minimal increases in stability.^{5–8} These reports may underestimate the increase because such systems often ignore aggregation and do not focus on stable native states.^{3,9} We have developed a simple system that provides information about the effects of macromolecular crowding on protein stability. Our system gives unambiguous data about the effects of a polymeric crowding agent on the stability of each residue in a globular protein. This quantitative information offers new insights into macromolecular stabilization of proteins.

We chose chymotrypsin inhibitor 2 (CI2) as our model globular protein because this protease inhibitor is small (7.5 kDa), amenable to biophysical study, and well-studied in terms of its structure, folding, and stability.^{10–12} More specifically, we used the I29A/I37H variant because the destabilizing isoleucine-to-alanine change¹³ allows stability measurements to be completed in 24 h and the histidine side chain provides an internal pH probe. We chose 40 kDa poly(vinylpyrrolidone) (PVP40) as the macromolecular crowding agent because this random-coil polymer is extremely soluble, has protein-like solution properties, and is metabolically inert.^{14,15} PVP has been widely used in pharmaceutical applications,^{16,17} and it retards both protein aggregation and proteolytic degradation,^{18–20} but its usefulness as a stabilizing agent for small proteins has never been investigated.

Materials and Methods

Protein Expression and Purification

The pet28a plasmid (Novagen) containing the gene for truncated wildtype CI2 was a gift from Dr. Andrew Lee (UNC). The first 19 residues of full length CI2 are disordered and are not included in this construct. Residue 20 of full-length CI2 is referred to here as residue 1. Site-directed mutagenesis was used to incorporate the I29A and I37H mutations. The forward primer for I29A was 5'GAA GCG CAG **GCA** ATC GTG C 3', where the changed codon is bold. The forward primer for I37H was 5' CT GCC GGT GGG **CAC** CCA TGT GAC CAT GGA ATA TC 3'. DNA sequence analysis (Genome Analysis Facility, UNC) with the T7 forward sequencing primer was used to confirm the sequence.

After sequence analysis, the plasmid was transformed into BL-21(DE3-Gold) competent *Escherichia coli* cells (Stratagene). The transformants were spread onto Luria broth agar plates containing 60 μ g/mL kanamycin (LB_{kan}). ¹⁵N-Enriched Spectra-9 media (25 ml, Spectra Stable Isotopes) was inoculated with a single colony and incubated overnight at 37 °C with shaking at 200 rpm. This overnight culture was diluted into 1 L of ¹⁵N-enriched Spectra-9 media in a 6 L autoclaved flask. The culture was grown at 37 °C with shaking at 200 rpm to an absorbance at 600 nm of 1.0. The cells were induced with isopropyl β -D-1-thiogalactopyranoside (Sigma) at a final concentration of 1 mM. The cells were harvested after 5 h by centrifugation at 7300 \times g in a swinging bucket centrifuge for 20 min.

The cell pellet was resuspended in 25 mL of 50 mM Tris buffer, pH 8.0. The slurry was sonicated (Fisher Scientific, Sonic Dismembrator Model 500) on ice (4 cycles, 4 min each, 30% duty cycle). The lysate was centrifuged at 20 000 \times g for 30 min. The pellet was discarded, and the supernatant was treated with a 10% solution of polyethyleneimine (final concentration 0.2%). After incubation on ice with stirring for 30 min, the precipitated nucleic acids were removed by centrifugation at 20 000 \times g for 30 min.

The clear lysate was loaded onto an anion-exchange column (Q Sepharose high performance resin, GE Healthcare, 1.6 cm \times 10 cm) connected to an AKTA FPLC (GE Healthcare) at 4 °C. The column was equilibrated with 25 mM Tris buffer, pH 8.0, before loading the sample. After loading, the column was thoroughly washed with 100 mL of 25 mM Tris, pH 8.0. CI2 does not interact strongly with the column material and was found in the flow-through and

wash. Purity was assessed by using SDS-PAGE on an 18% gel with Coomassie staining. If needed, the protein was further purified in H₂O by size-exclusion chromatography (HiLoad 16/60 Superdex 75 column, 1.6 cm × 60 cm, GE Healthcare) at 4 °C. The protein eluted between 80 and 100 mL. Protein concentration was determined by using the absorbance at 280 nm and an extinction coefficient of $7.04 \times 10^3 \text{ M}^{-1} \text{ cm}^{-1}$.²¹ Immediately following the purification, the protein was lyophilized and checked for structural changes by comparing chemical shifts with nonlyophilized protein. No significant change was observed. The typical yield of pure protein is 100 mg per 1 L culture.

NMR

For exchange experiments, the spectrometer was first shimmed by using a protein sample in acetate buffer, pH 5.4, at 37 °C. The exchange reaction mixture was prepared by dissolving lyophilized protein in 1 mL of 50 mM acetate buffer, pH 5.4, to a final concentration of 700 μM, followed by centrifugation and transfer of the supernatant to a 5 mm NMR tube. This buffer and those described below were made with 99.9% D₂O (Acros Organics). The sample was equilibrated in the spectrometer at 37 °C for 15 min before collecting the first spectrum. Consecutive HSQC spectra were collected for 24 h. The dilute-solution samples were saved for further experiments with GdmCl-induced denaturation. For the crowding study, lyophilized protein was resuspended in 50 mM acetate buffer, 300 g/L, 100 g/L, or 50 g/L PVP40, pH 5.4 to a final concentration of 800 μM. Shimming and data acquisition were performed as described above. The pH of each sample was checked before and after data collection. The reported pH value for deuterated solutions is uncorrected for the isotope effect. Peak volumes were obtained by using NMRView.²²

Measuring k_{ex} using CLEANEX-PM

The intrinsic rate of exchange (k_{ex}) for amide protons in the unprotected loop of the I29A/I37H variant was measured by using the water saturation transfer experiment, CLEANEX-PM.²³ Samples were prepared to a final concentration of 800 μM protein in 50 mM acetate buffer, pH 5.4 in the dilute solution, 300 g/L PVP40, or 100 g/L *N*-ethylpyrrolidone (NEP). The pH of each sample was determined before and after data collection. The data were collected on a Varian Inova 600 MHz spectrometer at 37 °C. The mixing times were 0, 10, 20, 40, and 53 ms for the dilute solution; 0, 10, 19, 25, and 53 ms for PVP40; and 0, 10, 19, 25, and 35 ms for NEP. NMR data were processed with NMRPipe²⁴ and analyzed with NMRView.²² Data were fitted as described by Hwang et al.²³

Results and Discussion

High concentrations of crowding agents might alter a globular protein's structure and aggregation state,²⁵ thereby confounding interpretation of their effects on stability. NMR chemical shifts are sensitive, empirical indicators of structure. We found PVP40-induced changes in ¹H and ¹⁵N backbone chemical shifts only in the loop and turn regions of CI2 (Figure S1, Supporting Information). Small changes in loops and turns are expected because crowding causes compaction, and unlike the protein core, loops are not by definition maximally compact.^{26,27} These chemical shift changes might also reflect weak interactions between PVP and these surface regions. We assessed the aggregation state of CI2 by quantifying the effect of PVP40 on the protein's extinction coefficient, ¹H and ¹⁵N resonance line-widths, and self-diffusion (Figures S2 and S3, Supporting Information). The extinction coefficient does not change in the 300 g/L PVP40 solution over the time required to conduct a stability measurement. Line widths in dilute solution and in 300 g/L PVP40 also remain constant, and the diffusion data are consistent with the monomeric nature of the protein in both dilute and crowded solutions. These results indicate that the combination of PVP40 and CI2 is amenable to stability studies.

We used amide-proton exchange to quantify stability. In our experiments, the protein is lyophilized and then redissolved in a D₂O-containing solution (buffer alone or buffer plus PVP40). The exchange rate of backbone amide protons for deuterons, k_{obs} , is quantified by measuring the decrease in the signal from individual amide protons in serially acquired NMR spectra over 24 h. The exchange reaction is described by eq 1.²⁸



The native state of the protein opens and closes with rate constants k_{op} and k_{cl} . Exchange occurs in the solvent-exposed open state with the rate constant k_{ex} . The generally accepted view is that the open states are ensembles whose subpopulations range from small, low amplitude fluctuations of the native state to rare, globally unfolded forms.^{29,30}

As shown in Figure 1, the 300 g/L PVP40 solution exhibits considerably slower exchange compared to the dilute solution. This result is consistent with crowding-induced stabilization, but quantitative analysis of protein stability requires information about the rate constants in eq 1.

The observed first-order rate constants for exchange at individual residues, k_{obs} , can be used to assess stability provided $k_{\text{op}}/k_{\text{cl}} \ll 1$ and $k_{\text{cl}} \gg k_{\text{ex}}$. Under these conditions,

$$k_{\text{obs}} = (k_{\text{op}}/k_{\text{cl}}) k_{\text{ex}} = K_{\text{op}}^{\text{oe}} k_{\text{ex}} \quad (2)$$

where $K_{\text{op}}^{\text{oe}}$ is the equilibrium constant for opening.³¹ Stability is measured as the free energy of opening, $\Delta G_{\text{op}}^{\text{oe}}$, where

$$\Delta G_{\text{op}}^{\text{oe}} = -RT \ln K_{\text{op}}^{\text{oe}} \quad (3)$$

and R is the gas constant and T is the absolute temperature. We know that $k_{\text{op}}/k_{\text{cl}} \ll 1$ for the slowly exchanging protons because independent unfolding experiments give $k_{\text{op}}/k_{\text{cl}} \approx 10^{-3}$ (Figure S4, Supporting Information). To show that $k_{\text{cl}} \gg k_{\text{ex}}$, we measured the pH dependence of k_{obs} .³¹ Exchange from the open state is acid/base catalyzed.³¹ Therefore, if $k_{\text{cl}} \gg k_{\text{ex}}$, plotting k_{obs} values at one pH against values at another pH will give a line of unitary slope.¹⁰ As anticipated, plots for experiments conducted in dilute solution and in 300 g/L PVP40 at two pH values (Figure 2) exhibit unitary slopes. The data show that $k_{\text{op}}/k_{\text{cl}}$ can be used to assess stability in dilute solution and in 300 g/L PVP40, but using eqs 2 and 3 to assess the effect of crowding requires knowledge of k_{ex} in dilute and crowded conditions.

Values of k_{ex} in dilute solution are computed from data on unstructured peptides.^{32–34} To assess the effect of 300 g/L PVP40 on k_{ex} , we used residue 37 in CI2's unprotected, extended loop (residues 35–45) as a mimic for an unstructured peptide. Exchange in the loop occurs too quickly to use the method described above, so we turned to the saturation transfer experiment, CLEANEX-PM.²³ Those data indicate that k_{ex} in 300 g/L PVP40 equals k_{ex} in dilute solution (Figure 3). With these data in hand, we calculated $\Delta G_{\text{op}}^{\text{oe}}$ values at each residue of CI2 and assessed the effects of crowding on stability.

A histogram of $\Delta G_{\text{op}}^{\text{oe}}$ values in dilute solution and 300 g/L PVP40 as a function of CI2 sequence position is shown in Figure 4, and $\Delta G_{\text{op}}^{\text{oe}}$ values are superimposed on the protein structure (PDB 2CI2) in Figure 5A and 5B. PVP40 increases $\Delta G_{\text{op}}^{\text{oe}}$ for all measurable residues with a maximum increase of ~ 3 kcal/mol, which corresponds to a 100-fold increase in the equilibrium constant

for folding ($1/K_{op}^{o'}$). This agrees with the predicted increases of 10- to 100-fold.¹ We attempted to confirm the maximum $\Delta G_{op}^{o'}$ values by performing a circular-dichroism-detected denaturation in PVP solutions supplemented with the denaturants guanidinium chloride or urea. Unfortunately, PVP interacts strongly with the cosolutes. Such behavior has been observed previously.¹⁶ Nevertheless, we feel our results are valid because the PVP concentration dependence of $\Delta G_{op}^{o'}$ values extrapolates smoothly to zero PVP concentration (*vide infra*), and many previous studies have shown correspondence between maximum $\Delta G_{op}^{o'}$ and free energies derived from global denaturation experiments.²⁹

To show the increases in $\Delta G_{op}^{o'}$ arise from the macromolecular nature of the crowding agent, we repeated the experiment in a solution of a model monomer for PVP, *N*-ethylpyrrolidone (NEP). CI2 precipitates in 300 g/L NEP but is soluble in 100 g/L NEP. At this concentration, k_{ex} , as measured with the CLEANEX-PM experiment, increases 4-fold compared to the dilute solution (Figure 3). We used this NEP-observed value to scale the calculated k_{ex} values. Values of $\Delta G_{op}^{o'}$ in 100 g/L NEP are overlaid on the protein structure in Figure 5C. NEP has a small effect, with most changes being destabilizing compared to the dilute solution. Higher NEP concentrations are expected to be even more destabilizing. These observations show that the stabilizing effect of PVP arises from its macromolecular nature and agrees with data showing that the effect of poly(ethylene glycol) on the overall stability of lysozyme exceeds the effect of PEG's monomer, ethylene glycol.³⁵

Measuring $\Delta G_{op}^{o'}$ on a residue-by-residue basis provides insight into the native and open states of CI2. Since the magnitude of $\Delta G_{op}^{o'}$ in the dilute solution depends on the amount of surface exposed upon unfolding,³⁶ it is expected, and observed (Figure 5A), that the smallest $\Delta G_{op}^{o'}$ values tend to correspond to surface-exposed residues and the largest values correlate with residues that become exposed only upon extensive unfolding. Identical patterns of local and global unfolding are observed in PVP40 and NEP compared to the dilute solution (Figure 5B and 5C). These data show that PVP40 significantly increases the stability of globally unfolding residues compared to the dilute solution and NEP while leaving the stability of locally unfolding residues nearly unchanged. From these observations, we conclude that crowding with PVP40 does not alter the exchange-competent forms (i.e., the open states) but decreases their probability.

Theories used to explain the effects of stabilizing (or destabilizing) cosolutes on protein stability predict that $\Delta G_{op}^{o'}$ should depend not only on differences in surface area but also on cosolute concentration.^{1,36–38} We expect a positive correlation between $\Delta G_{op}^{o'}$ values and the differential quantity, $\partial\Delta G_{op}^{o'}/\partial[PVP]$, which describes the sensitivity of $\Delta G_{op}^{o'}$ to PVP40 concentration. To test this idea we examined the effect of PVP40 concentration on $\Delta G_{op}^{o'}$ and mapped values of $\partial\Delta G_{op}^{o'}/\partial[PVP]$ onto the structure (Figure 5D). Comparing Figure 5B to Figure 5D shows exactly the correlation predicted by theory; residues with the largest $\Delta G_{op}^{o'}$ values have the largest $\partial\Delta G_{op}^{o'}/\partial[PVP]$ values.

Conclusion

We used a simple system comprising a globular protein, a random-coil polymer, and an established equilibrium thermodynamic method to quantify the stabilizing effects of macromolecular crowding at the level of individual residues. The maximum stabilizing effect is sizable, up to ~3 kcal/mol, which represents an increase in stability of ~50% compared to the dilute solution. Our residue-by-residue measurements show that crowding has the largest

effects on opening reactions that expose the most surface area but has little or no effect on regions that are solvent-exposed in both the native and open states. This observation reinforces the assertion that macromolecular crowding stabilizes the native state by destabilizing the unfolded states. This observation also suggests that information about turns and unstructured loops gained under equilibrium conditions in a dilute solution are valid under crowded conditions. Furthermore, the significant increase in protein stability as a result of crowding with a biocompatible polymer could lead to new approaches in the design and storage of protein pharmaceuticals.

Acknowledgements

We thank A. L. Lee for the CI2 expression system, T. G. Oas for helpful discussions, and E. T. Samulski and M. R. Redinbo for comments on the manuscript. L.C. and G.J.P. conceived the experiments; L.C., C.L., and G.B.Y. carried out the NMR experiments; C.O.B. measured the bulk stability; and L.C., J.O., and G.J.P. interpreted the data. This work was supported by G.J.P.'s NIH Director's Pioneer Award (5DP1OD783) and grants from the NSF (MCB 0516547) and the Petroleum Research Fund of the American Chemical Society (42748-AC4) to G.J.P. C.O.B. acknowledges the Research Education Support Program at the University of North Carolina at Chapel Hill and the Alliance for Graduate Education and the Professoriate (NSF HRD 9978874) for partial support during this project.

References

1. Minton AP. *Biophys J* 2005;88:971–985. [PubMed: 15596487]
2. Luby-Phelps KJ. *Int Rev Cytol* 2000;192:189–221. [PubMed: 10553280]
3. Minton AP. *J Pharm Sci* 2005;94:1668–1675. [PubMed: 15986476]
4. Sasahara K, McPhie P, Minton AP. *J Mol Biol* 2003;326:1227–1237. [PubMed: 12589765]
5. Ai X, Zhou Z, Bai Y, Choy WY. *J Am Chem Soc* 2006;128:3916–3917. [PubMed: 16551092]
6. Qu Y, Bolen DW. *Biophys Chem* 2002;10:101–102. 155–165.
7. Spencer DS, Xu K, Logan TM, Zhou HX. *J Mol Biol* 2005;351:219–232. [PubMed: 15992823]
8. van den Berg B, Wain R, Dobson CM, Ellis RJ. *EMBO J* 2000;19:3870–3875. [PubMed: 10921869]
9. Monterroso B, Minton AP. *J Biol Chem* 2007;282:33452–33458. [PubMed: 17878163]
10. Neira JL, Itzhaki LS, Otzen DE, Davis B, Fersht AR. *J Mol Biol* 1997;270:99–110. [PubMed: 9231904]
11. Jackson SE, Fersht AR. *Biochemistry* 1991;30:10428–10435. [PubMed: 1931967]
12. Itzhaki LS, Neira JL, Fersht AR. *J Mol Biol* 1997;270:89–98. [PubMed: 9231903]
13. Jackson SE, Moracci M, elMasry N, Johnson CM, Fersht AR. *Biochemistry* 1993;33:11259–11269. [PubMed: 8218191]
14. Ravin HA, Seligman AM, Fine J. *New Engl J Med* 1952;247:921–929. [PubMed: 13002648]
15. Klech CM, Cato AE III, Suttle AB III. *Colloid Polym Sci* 1991;269:643–649.
16. Lukyanov AN, Torchilin VP. *Adv Drug Delivery Res* 2004;56:1273–89.
17. Rogero SO, Malmonge SM, Lugao AB, Ikedo TI, Miyamaru L, Cruz AS. *Artif Organs* 2003;27:424–427. [PubMed: 12752201]
18. O'Malley JJ, Ulmer RW. *Biotechnol Bioeng* 1973;25:917–925. [PubMed: 4748853]
19. Gombotz WR, Pankey SC, Phan D, Drager R, Donaldson K, Antonsen KP, Hoffman AS, Raff HV. *Pharm Res* 1994;11:624–632. [PubMed: 8058628]
20. Kamada H, Tsutsumi Y, Yamamoto Y, Kihira T, Kaneda Y, Mu Y, Kodaira H, Tsunoda SI, Nakagawa S, Mayumi T. *Cancer Res* 2000;60:6416–20. [PubMed: 11103807]
21. Roesler KR, Rao AG. *Protein Eng* 1999;12:967–973. [PubMed: 10585502]
22. Johnson BA, Blevins RA. *J Biomol NMR* 1994;4:603–614.
23. Hwang TL, van Zijl PCM, Mori S. *J Biomol NMR* 1998;11:221–226. [PubMed: 9679296]
24. Delaglio F, Grzesiek S, Vuister GW, Zhu G, Pfeifer J, Bax A. *J Biomol NMR* 1995;6:277–293. [PubMed: 8520220]
25. Minton AP. *Mol Cell Biochem* 1983;55:119–140. [PubMed: 6633513]
26. Perham M, Stagg L, Wittung-Stafshede P. *FEBS Lett* 2007;581:5065–5069. [PubMed: 17919600]

27. Stagg L, Zhang SQ, Cheung MS, Wittung-Stafshede P. Proc Natl Acad Sci USA 2007;104:189671–18981.
28. Hvidt A, Nielsen SO. Adv Protein Chem 1966;21:187–386.
29. Clarke J, Itzhaki LS. Curr Opin Struct Biol 1998;8:112–118. [PubMed: 9519304]
30. Woodward CK, Hilton BD. Biophys J 1980;32:561–575. [PubMed: 7248461]
31. Englander SW, Kallenbach NR. Q Rev Biophys 1983;16:522–655.
32. Sphere (<http://www.fccc.edu/research/labs/roder/sphere/sphere.html>).
33. Zhang, YZ. Protein and peptide structure and interactions studied by hydrogen exchange and NMR thesis. University of Pennsylvania; 1995.
34. Bai Y, Milne JS, Mayne L, Englander SW. Proteins 1993;17:75–86. [PubMed: 8234246]
35. Tokuriki N, Kinjo M, Negi S, Hoshino M, Goto Y, Urabe I, Yomo T. Protein Sci 2004;13:125–133. [PubMed: 14691228]
36. Bai Y, Sosnick TR, Mayne L, Englander SW. Science 1995;269:192–196. [PubMed: 7618079]
37. Timasheff SN. Proc Natl Acad Sci USA 2002;99:9721–9726. [PubMed: 12097640]
38. Baldwin RL. J Mol Biol 2007;371:283–301. [PubMed: 17582437]

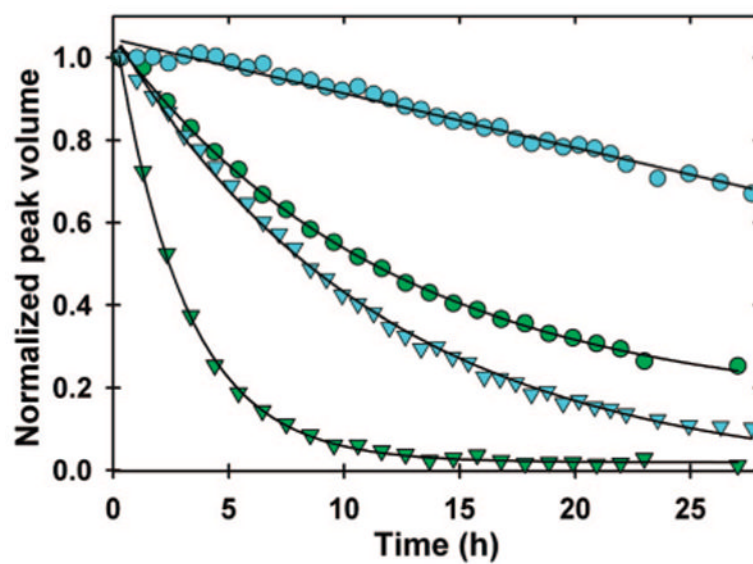


Figure 1. PVP40 slows amide proton exchange. Exchange curves for the amide protons of Leu 32 (●) and Asp 52 (▼) in dilute solution (green) and 300 g/L PVP40 (cyan). Conditions: 50 mM acetate buffer in D₂O, pH 5.4, 37 °C.

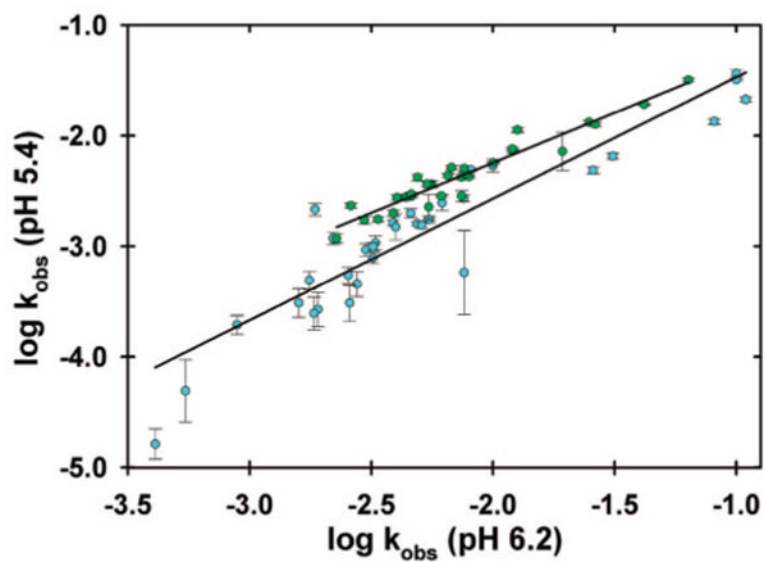


Figure 2.

The I29A/I37H variant exchanges according to the EX2 mechanism. Linear regression yields slopes and R^2 values of 0.91 ± 0.5 and 0.92 in dilute solution (green) and 1.10 ± 0.08 and 0.86 in 300 g/L PVP40 (cyan), respectively. The error bars represent the standard errors for the averages from three trials collected at pH 5.4.

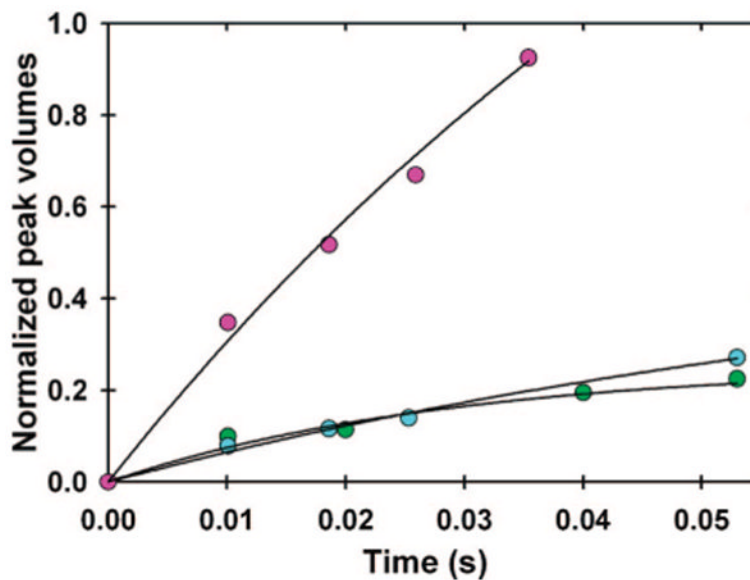


Figure 3.

Crowding with 300 g/L PVP40 does not change exchange rate for loop residue 37, which is essentially unprotected, but adding 100 g/L NEP increases the rate approximately 4-fold. The exchange of residue 37 was measured in 50 mM acetate, pH 5.4 at 37 °C in 300 g/L PVP40 (cyan), in dilute solution (green), and in 100 g/L NEP (magenta) using the CLEANEX-PM experiment.²³ The rate is $9 \pm 2 \text{ s}^{-1}$ in dilute solution, $7 \pm 1 \text{ s}^{-1}$ in PVP40, and $32 \pm 3 \text{ s}^{-1}$ in NEP. The smooth curve is determined as described by Hwang et al.²³

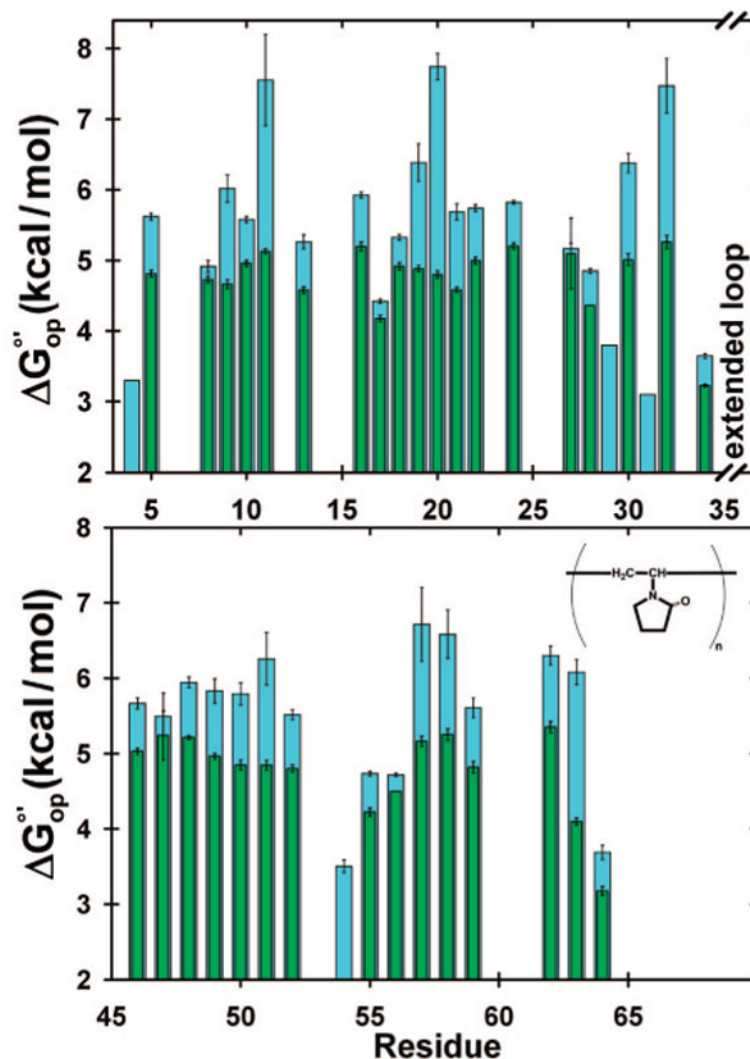


Figure 4.

Macromolecular crowding with PVP40 stabilizes the I29A/I37H variant of CI2 relative to dilute solution. Values of ΔG_{op}° in 300 g/L PVP40 (cyan) and dilute solution (green) are plotted versus residue number. The height of each bar represents the average from three trials. The error bars represent the standard deviation. Conditions: 700–800 μM variant protein, 50 mM acetate buffer in D_2O , pH 5.4. The inset shows the backbone structure of PVP.

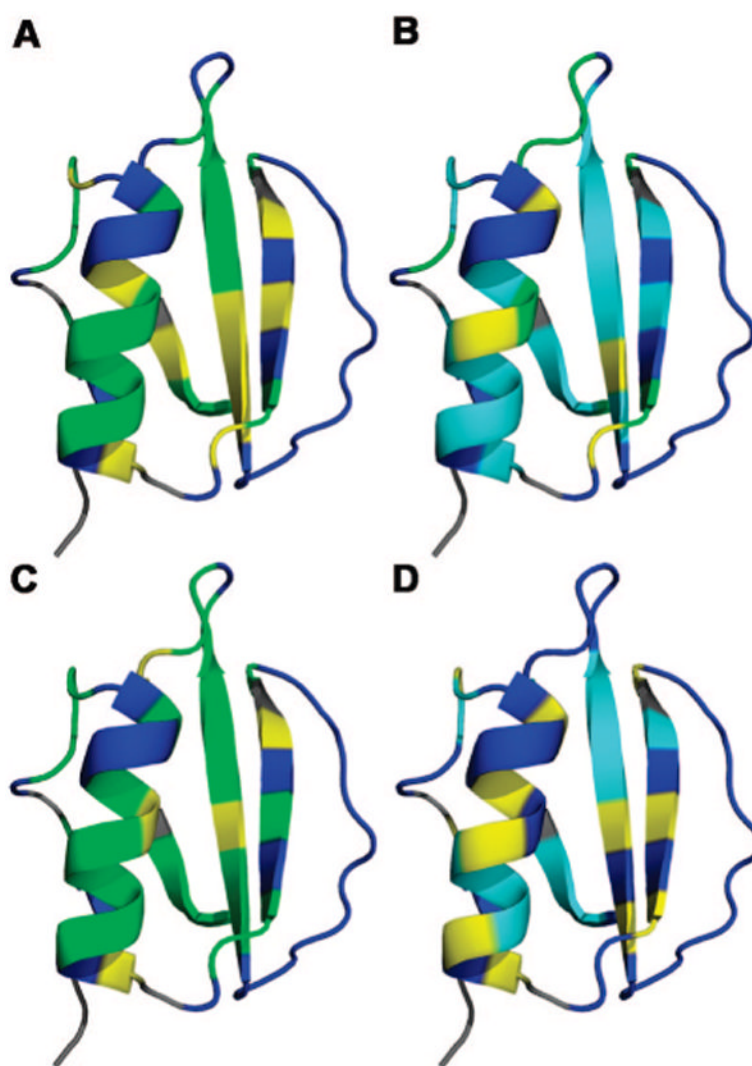


Figure 5.

Ribbon structure of wild-type CI2 (PDB, 2CI2) colored by $\Delta G_{op}^{o'}$ for the I29A/I37H variant in (A) dilute solution, (B) 300 g/L PVP40, and (C) 100 g/L NEP [blue: $\Delta G_{op}^{o'} < 3.0$ kcal/mol; green: $3.0 \text{ kcal/mol} < \Delta G_{op}^{o'} < 5.0$ kcal/mol; yellow: $5.0 \text{ kcal/mol} < \Delta G_{op}^{o'} < 5.5$ kcal/mol; cyan: $5.5 \text{ kcal/mol} < \Delta G_{op}^{o'} < 8.0$ kcal/mol]. (D) $\Delta G_{op}^{o'}$ was measured in 0, 50, 100, and 300 g/L PVP40, and $\delta\Delta G_{op}^{o'}/\delta[\text{PVP40}]$ Values were superimposed onto the structure [blue: $\delta\Delta G_{op}^{o'}/\delta[\text{PVP40}] = 0$; yellow: $0 < \delta\Delta G_{op}^{o'}/\delta[\text{PVP40}] < 2.5 \times 10^{-3}$ (kcal/mol)/M; cyan: $2.5 \times 10^{-3} \text{ (kcal/mol)/M} < \delta\Delta G_{op}^{o'}/\delta[\text{PVP40}] < 1.0 \times 10^{-2}$ (kcal/mol)/M]. Residues for which there are no data are colored gray.